Morphology De-ringing Filter Design for Ultrasound Images

Yen-Yu Chen
Institute of Electrical Engineering
National Cheng Kung University
miscyy@tcts1.seed.net.tw

Shen-Chuan Tai
Institute of Electrical Engineering
National Cheng Kung University
sctai@mail.ncku.edu.tw

Abstract

Various medical image compression techniques have been proposed for accelerating image propagation in many applications. JPEG2000 is a new generation technique that can encode near lossless ultrasound images at medium bit-rate with diagnostically acceptable quality. Because the coder of JPEG2000 is based on wavelet transform, the reconstructed image will contain some ringing artifacts. Some de-ringing algorithm must be applied to enhance image quality. This study presents quad-tree decomposition and a set of morphological filters for reducing the ringing artifacts of ultrasound images. Specifically, the presented morphological filters use eight predefined morphological operations, including four structuring elements (SE) that include both dilation and erosion. The proposed voting strategy can be used to select the morphological filter for each block to optimize decoded image quality. Image quality can be enhanced by applying the appropriate morphological filter to each block. Experimental results demonstrate that the proposed technique enhances reconstructed ultrasound image quality compared to JPEG2000 at the same bit rate in terms of both PSNR and the perceptual results.

Keywords: JPEG2000, ringing artifacts, morphological filter

1. Introduction

The development of digital image processing and network technology has led to various images being stored and transmitted digitally, including medical images. However, limitations of network bandwidth and storage capacity make compression necessary in storing and transmitting digital images. Considerable fidelity loss, namely compression ratio of about 40:1 or even 100:1, generally is acceptable in compression [1]. However, for medical images [2][3][4][5][6][7][8] diagnostic concerns limit compression ratio.

Digital medical images are important in diagnosis. Ultrasound images, a popular medical image modality, have distinguishing features that must be preserved during compression. Typical ultrasound images comprise an ultrasound-scanned area, which often is nonrectangular, and a background containing text and limited graphics. Speckled texture is an important feature of ultrasound images. However, since speckles become blurred at medium bit-rate compression, the tradeoff between speckle preservation and compression ratio becomes a core problem. Speckle preservation also is important for radiologists since they are accustomed to working with speckled images, meaning that noticeable image distortion should be avoided.

Algorithms based on the wavelet transform [9] are the current state of the art in image compression. One of the most representative wavelet-based image coding algorithms is set partitioning in hierarchical trees (SPIHT) [10], which is a refined version of the embedded zero-tree algorithm (EZW) [11]. One study concluded that wavelet-based methods such as SPIHT are subjectively superior to JPEG compressed at moderately high bit-rate [12]. However, SPIHT developed ringing artifacts at rates above 12:1, impacting diagnostic acceptability. The new still image compression standard JPEG2000 [13], another wavelet-based image coding algorithm, provide better quality than SPIHT at low bit-rate and generally performs better. Images coded at medium bit-rate suffer from loss of detail and sharpness, as well as various coding artifacts. Ringing, one of the coding artifacts, appears as small ripples around the edge of the image. To achieve sufficient image quality for medium bit-rate wavelet-based image coding, post-processing efficiently improves compression results. Additionally, post-processing considers original image, meaning it can preserve medical image fidelity.

A few de-ringing algorithms have been proposed recently and are described in detail in [14][15][16]. The de-ringing algorithm proposed by Shen and Kuo [16], which is also described in JPEG2000 VM 7.0 [13], is considered a suitable post-processor for JPEG2000. The de-ringing algorithm replaces each pixel value with a function of the values of neighboring pixels that are within a specified window. To avoid conflict with the above goal, that is smooth shade regions and sharp edges, the de-ringing algorithm uses a number of adaptive noise reduction algorithms. Essentially, the de-ringing algorithm attempts to detect edges in the image in a different way to preserve them. Shen and Kuo also introduced the idea of image ringing artifact reduction through nonlinear filtering by using different kinds of potential functions.

2. Proposed Post-processing Method

Medical image compression ratio thus usually is low, meaning that processing and transmitting the huge amount of image data involved in a medical image processing system frequently is time consuming. Hence, this study proposed a post-processing algorithm to suppress the compression artifact of the ultrasound images and maximize compression ratio and image fidelity. The proposed post-processing algorithm consists of quad-tree decomposition, and morphology based filtering, as described in the following subsections.

A. Quad-tree decomposition

Since the ringing artifacts appear mostly in edge and texture areas, a criterion is needed for identifying smooth or textured regions on an image. This work adopts the quad-tree partition scheme, which is efficient and block-based, to pre-process the compressed image. The main purpose of the quad-tree partition is to enable the post-processing method to focus the local feature of the compressed image to promote global image quality. Initially, a threshold is required to classify block smoothness and set a minimum block size to stop the partition. To determine block smoothness, this study simply calculates the absolute difference between the maximum and minimum gray value in a block. If this absolute difference exceeds the pre-defined threshold, the block is divided into four half-sized sub-blocks. Partition processing is repeated in each block until the smoothness meets the defined criterion or the block size equals the previously defined minimum size.

Following quad-tree partition, the image is divided into different sized blocks according to its features. In large blocks, namely 8 x 8 or larger, the gray-scale value of the block is almost the same. The main concern of this study is that the features of small blocks, that is, 4 x 4 and 2 x 2, may contain important information for ultrasound images, such as edge, texture, and ringing artifacts. Applying a morphology based filter to these small blocks would reduce ringing around the edge while maintaining and reconstructing edge detail. Figure 1 shows an example of a quad-tree partition in a ring image 'sonogram'.

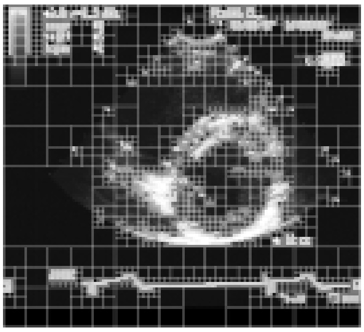

Fig. 1. Quad-tree partition in the ringing image 'sonogram'.

B. Morphology based filtering

After dividing the compressed medical image into various size blocks, the main operation of the post-processing algorithm can be performed efficiently. In each block, morphology based filtering is performed to enhance image quality. The most helpful structuring element (SE) and morphology operation is evaluated using the absolute difference between the filtered and original image blocks. The most helpful type of morphological operation is that which maximizes the reduction of the absolute difference between the filtered image block and the original image. The gray scale morphology defines gray scale dilation as an operation that selects the maximum pixel value from the mask window (the same dimension as the SE) provided that the corresponding element in the SE window is one. Similarly, gray scale erosion is defined as an operation that selects the smallest pixel value from the mask window provided that the corresponding element in the SE window is one.

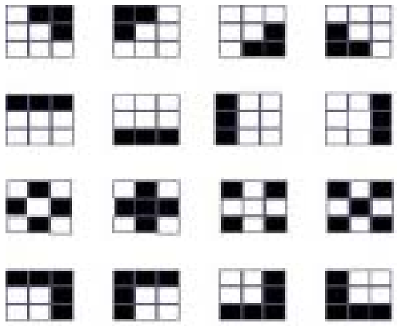

Fig.2. The 16 pre-specified Ses.

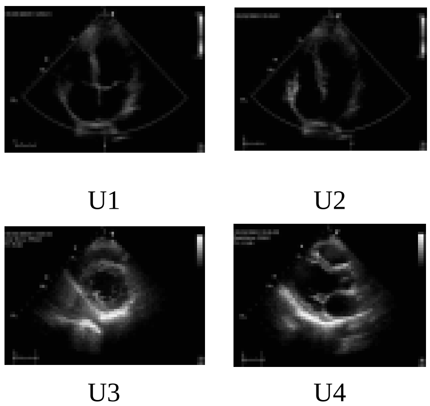

Fig. 3. Four 434*636 left atria images.

To reduce the complexity and computation time, this study only considers 3x3 SEs and dilation and erosion. This study uses 16 pre-specified SEs, as shown in Fig. 2, taken by 16 different directions, and measures their contribution to improving PSNR. For the wavelet-based encoded image, this work calculated the statistical properties of improvement for 100 test images (Fig. 3 illustrates four 434*636 left atria images) and Table 1 lists the results. Data analysis yields the following guidelines for filter design. Importantly, the experimental results show that SE1 to SE8 can enhance ringing image quality and that each SE can improve specific features of the ringing image. The filtering can select the four SEs that achieve the biggest improvement in PSNR.

The post-processing algorithm can be summarized as follows:

At the encoder end:

Input: Original image ***P***, ringing image ***P'***, quad-tree partition threshold, minimum block dimension, and morphological operations (four SEs with both dilation and erosion) OP(1) ~ OP(8).

Output: Side information for de-ringing.

Step 1. Partition ***P*** and ***P'*** into unequal-sized blocks using quad-tree, calculate the absolute difference of every block, Diff(i) = abs(***P***(i) – ***P'***(i)) , where ***P***(i) & ***P'***(i) are the corresponding blocks in ***P*** & ***P'***.

Step 2. Select an unprocessed block ***P'***(i) and perform all eight morphological operations. Then save the morphological results following the eight operations, say $MP'(1) \sim MP'(8)$.

Step 3. Sort $MP'(k)$ by $\sum_j \mathrm{abs}(MP_j'(k) - P_j(i))$, where j stands for pixel in a given block, select the smallest $MP'(k)$, and check whether the block error is smaller than Diff(i). If so, record the filter number. Otherwise, leave the block unchanged.

Step 4. Repeat from step 2 until all blocks are processed.

Step 5. Compress the filter information by entropy coding.

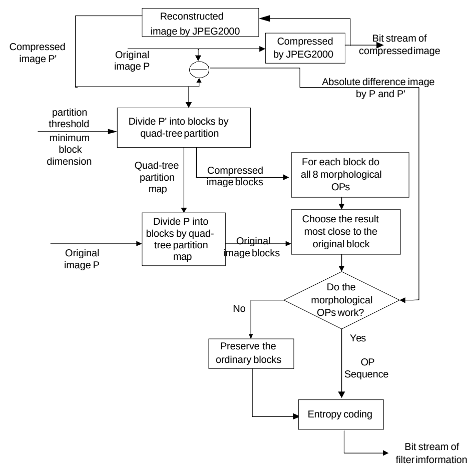

Fig. 4. Flowchart of de-ringing encoder.

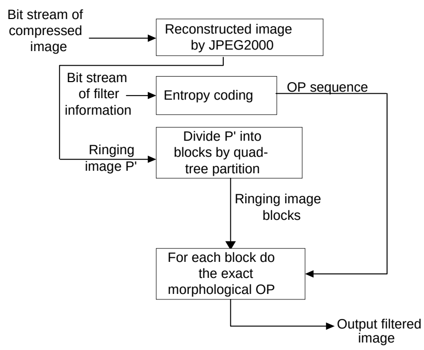

Fig. 5. Flowchart of de-ringing decoder.

At the decoder end:

Input: Ringing image ***P'***, threshold of quad-tree partition, minimum block dimension, and morphological operations OP(1) ~ OP(8)

Output: Filtered image ***Q***

Step 1. Copy ***P'*** to ***Q***.

Step 2. Partition ***P'*** into unequal-sized blocks using quad-tree as done by the de-ringing encoder.

Step 3. Select an unprocessed block ***P'***(i) and apply the exact morphological filter to it. Assume that the filtered block is

MP'(*k*).

Step 4. Replace the corresponding block in ***Q*** with *MP'*(*k*). However, if the side information of this block indicates that no suitable pre-defined filter exists, leave the block unchanged.

Step 5. Repeat from step 3 until all blocks are processed.

Figures 4 and 5 illustrate the flowchart of the de-ringing encoder and decoder, respectively.

3. Simulation results

Fig. 6 (a)

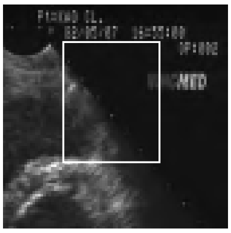

Fig. 6(b)

Fig. 6(c)

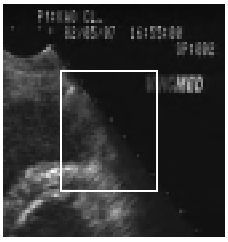

Fig. 6(d)

Fig. 6 (a) Original sonogram1.
(b)Ringing image compressed by JPEG2000(bit rate = 0.5321, PSNR=36.31 dB).
(c)Ringing image compressed by JPEG2000(bit rate = 0.5, PSNR=36.14 dB).
(d) Filtered image of Fig. 6(c)(bit rate=0.5321, PSNR=36.91 dB)

This investigation conducted some experiments on the 512 x 512 grayscale ultrasound image with 8 bits per pixel. The ultrasound image was compressed by JPEG 2000 at bit-rate of 0.1 to 0.6 bpp. The minimum block size was set to 2 for a partition threshold of 60 and 4 for a partition threshold of 20. The two parameters of the quad-tree decomposition were determined by an empirical experiment with respect to side information size and morphological filter performance. Moreover, the side information was compressed using adaptive Huffman coding to further reduce total bit-rate. As is known, a better artifact-free image can be obtained using a small partition threshold and minimum block size. On the other hand, such a set up is associated with a heavy load of side information. Therefore, this study sets the partition threshold and minimum size as 20, 4, and 60, 2 respectively throughout the experiment.

This work displays some images filtered by the proposed method. For clarity, only the most complicated quarters of the whole images are displayed here, namely the images are truncated to figures of 256 by 256. In Fig. 6, those complicated images include the original image, the ringing images (compressed by JPEG2000), and the filtered image. Notably, the visual quality of the ringing images also is enhanced.

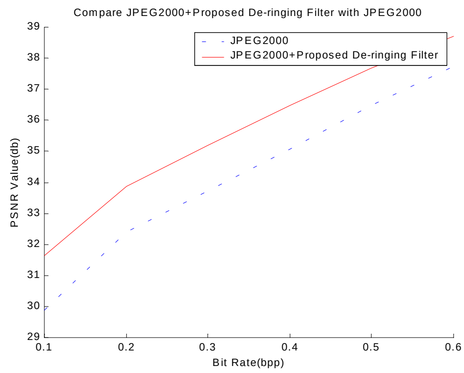

Fig. 7. Statistical summary of 100 ultrasound images of the left atria.

For comparative purposes, this study also lists the related compression results of JPEG2000 in Table 2. The total consumed bit-rate is recalculated to include the side information. Fig. 7 statistically summarizes 100 ultrasound images of the left atria. From the summarized results, the ultrasound image can be compressed almost without loss while preserving key detail using the post-processing algorithm.

The side information can successfully solve the problem of compressing ultrasound images at medium bit-rate. Additionally, the fidelity of the total bit-rate is more acceptable diagnostically than the same bit-rate compressed by JPEG2000.

4. Conclusions

The wavelet transform-based image compression algorithm achieves superior performance to JPEG. Moreover, the new still image compression standard, JPEG 2000, is superior to JPEG in dealing with the transmission and storage of various images. Reducing storage requirements and increasing data transfer efficiency are two reasons for applying compression to ultrasound images. However, ultrasound images have some distinguishing features that need special attention during compression. When ultrasound images compressed at medium bit-rate, about 0.4 to 0.6, by JPEG2000, the quality is near distortion free and image quality appears to remain unchanged. As the compression ratio exceeds 12:1, the compressed images develop ringing artifacts, impacting diagnostic acceptability. This work designs the post-processing algorithm, which successfully enhances the quality of ultrasound images coded near lossless. Using the side information, the ultrasound images coded at medium bit rate also can achieve acceptable quality.

The proposed de-ringing filter is more simple and effective than methods implemented on the frequency domains [14] [15]. Owing to its low complexity, the proposed filter is very suitable for hardware implementation. Moreover, in JPEG2000 VM 7.0 de-ringing filter, another previously developed method significantly traduced the visual quality of ringing artifacts. However, PSNR improves insignificantly and in fact can even decline after the ringing artifacts are removed using their proposed strategy. For removing ringing artifacts from ultrasound images, the proposed approach can significantly improve the quality of the reconstructed images, in terms of both visual inspection and PSNR. Also, the fidelity preservation of the proposed de-ringing method makes it a promising approach for stretching the wavelet compression of ultrasound images to lower bit-rates.

Acknowledgement

This research is supported partially by the National Science Council of Taiwan under the contract number of NSC 92-2213-E-006-081

References

[1] A. K. Jain, “Image data Compression: A review,” in *Proc. IEEE*, vol. 69, pp. 349-389, 1981.

[2] Digital imaging and communication in medicine (DICOM), version 3, American College of Radiology (ACR) / National Electrical Manufacturers Association (NEMA) Standards Draft, Dec. 1992.

[3] R. C. Gonzalez and R. E. Woods, Digital Image Processing, Addision-Wesley, Reading, MA, 1992.

[4] S. Wong, L. Zaremba, D. Gooden, and H. K. Huang, “Radiologic Image Compression - a review,” *Proc. IEEE*, vol. 83, no.2, pp. 194-219, 1995

[5] Y. G. Wu and S. C. Tai, “Medical Image Compression by Discrete Cosine Transform Spectral Similarity Strategy,” *IEEE Trans. Information Technology in Biomedicine*, vol. 5, no. 3, pp. 236-243, Sep. 2001.

[6] J. Wang, and H. K. Huang, “Medical Image Compression by Using Three- Dimensional Wavelet Transformation,” *IEEE Tran. Medical Imaging*, vol. 15, no. 4, Aug. 1996.

[7] A. Baskuet, H. Benoit-Cattin, and C. Odet, ”On a 3-D medical image coding method using a separable 3-D wavelet transform,” *SPIE Med. Imag*., vol. 2431, pp. 173-183, 1995.

[8] S. C. Lo, J. Xuan, H. Li, M. T. Freedman, and S. K. Mun, “Arithmetic Wavelet Decompositions in Radiological Image Compression,” *Proc. SPIE Medical*

Imaging Conference, 3031, 1997.
[9] M. Antonini, N. Barlaud, P Mathieu and I. Daubechies, ”Image coding using wavelet transform”, *IEEE Trans. Image Processing*, vol. 1, pp. 205-220, Apr.1992.
[10] A. Said and W. A. Pearlman, “A new, fast, and efficient image codec based on set partitioning in hierarchical trees,” *IEEE Trans. Circuits and System for Video Technology*, vol. 6, no. 3, pp. 243-250, Jun. 1996.
[11] J. Shapiro, “Embedded image coding using zerotrees of wavelet coefficients,” *IEEE Trans. Signal Processing*, vol. 41, pp. 3445-3462, Dec. 1993.
[12] Ed Chiu, Jacques Vaisey, and M. Stella Atkins, “Wavelet-based space-frequency compression of ultrasound images,” *IEEE Trans. Information Technology in Biomedicine*, vol. 5, no. 4, pp. 300-310, Dec. 2001.
[13] “JPEG2000 Verification Model 7.0”, ISO/IEC JTC 1/SC 29/WG 1 N1684, Apr. 2000.
[14] Tariq Bakir and Stanley J. Reeves, “A filter design method for minimizing ringing in a region of interest in MR spectroscopic images,” *IEEE Tran. Medical Imaging*, vol. 19, no. 6, pp. 585-600, Jun. 2000.
[15] Rick Archibald and Anne Gelb, “A method to reduce the Gibbs ringing artifact in MRI scans while keeping tissue boundary integrity,” *IEEE Tran. Medical Imaging*, vol. 21, no. 4, pp. 305-319, Apr. 2002.
[16] Mei-Yin Shen and C.-C. Jay Kuo, “Artifact reduction in low bit rate wavelet coding with robust nonlinear filtering,” *IEEE Second Workshop on Multimedia Signal Processing*, pp. 480-485, 1998.

Table 1: Statistical summary of the improvement of each structural element.

Improvement of structural elements								
Image	**SE1**	**SE2**	**SE3**	**SE4**	**SE5**	**SE6**	**SE7**	**SE8**
U1	0.090	0.110	0.110	0.090	0.090	0.080	0.140	0.120
U2	0.100	0.090	0.130	0.120	0.130	0.100	0.120	0.110
U3	0.120	0.100	0.110	0.100	0.100	0.090	0.140	0.100
U4	0.080	0.080	0.070	0.080	0.070	0.060	0.090	0.070
Average PSNR of four left atria images in Fig. 3.	0.098	0.095	0.105	0.098	0.098	0.083	0.123	0.100
Average PSNR of 100 left atria images.	0.095	0.096	0.103	0.097	0.101	0.082	0.125	0.104
Image	**SE9**	**SE10**	**SE11**	**SE12**	**SE13**	**SE14**	**SE15**	**SE16**
U1	0.020	0.002	0.030	0.004	0.020	0.030	0.020	0.010
U2	0.040	0.001	0.040	0.005	0.020	0.020	0.030	0.020
U3	0.020	0.001	0.030	0.003	0.020	0.020	0.010	0.020
U4	0.020	0.001	0.020	0.003	0.010	0.010	0.010	0.010
Average PSNR of four left atria images in Fig. 3.	0.025	0.001	0.030	0.004	0.018	0.020	0.018	0.015
Average PSNR of 100 left atria images.	0.026	0.001	0.028	0.005	0.015	0.021	0.016	0.014

Table 2: Experiments on total bit-rate and PSNR with sonogram1.

Bit-rate (bpp)	**PSNR of JPEG2000 (dB)**	**Partition threshold**	**Minimum block size**	**Total consumed bit-rate (bpp)**	**PSNR of JPEG2000 + proposed de-ringing filter (dB)**	**PSNR of same bit-rate JPEG2000 (dB)**	**PSNR of JPEG2000 + VM7.0 filter (dB)**
0.1	28.77	60	2	0.1531	32.30	30.33	30.04
		20	4	0.1452	32.21	30.17	29.94
0.2	31.91	60	2	0.2506	34.56	32.72	32.52
		20	4	0.2431	34.31	32.68	32.52
0.3	33.88	60	2	0.3442	35.71	34.41	34.27
		20	4	0.3401	35.52	34.30	34.23
0.4	35.19	60	2	0.4392	36.49	35.46	35.36
		20	4	0.4366	36.35	35.44	35.38
0.5	36.14	60	2	0.5353	36.99	36.32	36.26
		20	4	0.5321	36.91	36.31	36.27
0.6	36.92	60	2	0.6314	37.60	37.04	37.01
		20	4	0.6292	37.52	37.00	36.98